Thermoelectric Properties of $Ag_8Ge_{1-x}Mn_xTe_6$ Solid Solutions

© R.N. Rahimov[1], A.S. Qahramanova[1], D.H. Arasly[1], A.A. Khalilova[1], I.Kh. Mammadov[2], A.R. Khalilzade[3]

[1] Institute of Physics, National Academy of Sciences of Azerbaijan,
AZ1143 Baku, Azerbaijan
[2] Azerbaijan State Aviation Academy,
AZ1045 Baku, Bina, Azerbaijan
[3] University of Waterloo, 200 University Ave W, Waterloo,
ON N2L 3G1, Canada

E-mail: rashad@physics.science.az

Received November 18, 2021
Revised January 18, 2022
Accepted June 10, 2022

$Ag_8Ge_{1-x}Mn_xTe_6$ solid solutions with different manganese content ($x = 0$, 0.05, 0.1, 0.2) were prepared by alloying and further pressing the powders under a pressure of 0.6 GPa. By the X-ray diffraction studies have shown that the introduction of manganese atoms leads to the compressibility of the Ag_8GeTe_6 lattice. All *p*-type samples had high resistance below the transition at temperatures of 180−220 K. An increase in electrical conductivity in the range of 220−300 K was analyzed using the Mott ratio; at temperatures $T > 320$ K, semiconductor behavior is observed in all compositions. The highest thermoelectric figure of merit $ZT = 0.7$ at 550 K was obtained for a solid solution of the composition $Ag_8Ge_{1-x}Mn_xTe_6$ ($x = 0.05$).

Keywords: solid solution, $Ag_8Ge_{1-x}Mn_xTe_6$, thermoelectric efficiency, amorphization, low thermal conductivity

DOI: 10.21883/SC.2022.09.54129.9760

1. Introduction

The conversion of energy losses into electric energy with the use of thermoelectric converters is a topical issue. Materials with a high Seebeck coefficient (S), a high electric conductivity (σ), which helps achieve a high power factor ($\alpha^2\sigma$), and a low thermal conductivity (k), which should reduce the heat flow at transition points, are needed to construct thermoelectric generators [1]. The conductivity and the Seebeck coefficient are critical parameters of thermoelectric materials, and the thermal conductivity is considered key to converters. Therefore, the search for materials with a low thermal conductivity is relevant to current studies. Research suggests that fine thermoelectric materials are often heavily doped semiconductors by nature with a carrier density from 10^{19} to 10^{21} cm^3 [2]. The thermal conductivity of most semiconductors is high, since the free path length of phonons exceeds the lattice constant. A disturbance of periodicity or emerging defects scatter phonons, thus reducing their free flux and, consequently, the thermal conductivity. It was found that ionic crystals (mixed conductors) may also serve as thermoelectric materials due to their extremely low lattice thermal conductivity [3,4]. Owing to a complex crystal structure and a large lattice cell, ternary ionic compound Ag_8GeTe_6 features a number of unusual properties: a low thermal conductivity and a small band gap [5–8]. This compound exhibits superionic conductivity and is considered to be a perfect material both for conversion of heat into electricity and for storage of electricity [9–11]. Owing to its elevated molar heat capacity (30 J/mol-K at room temperature), Ag_8GeTe_6 is an unstable system, a mixed conductor with a low thermal conductivity. The authors of [11] obtained a nonstoichiometric composition of this material and thus managed to reduce its thermal conductivity and raise the thermoelectric efficiency. The suppression of thermal conductivity was attributed to vitrifaction or amorphization of the phonon system in Ag_8GeTe_6.

It is known that the parameters of a solid solution and the temperature of phase transitions in it may be adjusted by varying its composition. Impurity atoms contained in an alloy disturb the potential field and periodicity in the crystal. A deformation region, which distorts the crystal lattice, forms around defects and impurity atoms. Such defects in ionic crystals reduce the free path length of phonons further, thus resulting in a low thermal conductivity. In the present study, new alloys were prepared by adding highly soluble and diffusional manganese to ternary compound Ag_8GeTe_6. Manganese was chosen largely to obtain *p*-type conductivity. Being a magnetic impurity, Mn also induces a greater lattice distortion and, consequently, a reduction in thermal conductivity. Its influence on the kinetic parameters of solid solution $Ag_8Ge_{1-x}Mn_xTe_6$ and on the thermoelectric figure of merit was examined.

2. Experiment

Solid solutions $Ag_8Ge_{1-x}Mn_xTe_6$ with different manganese concentrations ($x = 0$, 0.05, 0.1, 0.2) were obtained by alloying [10]. The synthesized material was ground, sifted, and pressed in a parallelepiped steel dresser under a pressure of 0.6 GPa. The obtained iron-grey samples $15 \times 5 \times 2$ mm in size were homogenized at ~ 800 K for 10 h.

X-ray diffraction and microstructure analyses were carried out to characterize the samples. A Bruker D2 Phaser diffractometer was used to perform the diffraction analysis at angles $5 \le 2\theta \le 80°$ with Cu$-K_\alpha$ radiation. The microstructure and elemental analysis was performed with a JEOL 6610LV electron microscope fitted with an energy dispersive X-ray spectroscopy (EDX) system. The electric conductivity and the thermal emf were examined in the 80–700 K temperature range using the compensation method and contact tungsten probes. Temperature dependences of the temperature conductivity were measured under pulsed light heating [12]. A photoflash with a power of 120 J and a flash duration of 10^{-3} s was used in measurements. A quartz light guide was positioned between the sample and the photoflash.

3. Results and discussion

The diffraction patterns for solid solution $Ag_8Ge_{1-x}Mn_xTe_6$ ($x = 0$, 0.05, 0.1, 0.2) demonstrated that the obtained solutions are identical in structure to Ag_8GeTe_6 (Fig. 1), but the reflections shift noticeably toward smaller angles at an Mn concentration of 10 and 20% (i.e., the introduction of manganese atoms induces lattice compressibility [13]. All reflections of the $Ag_8Ge_{0.8}Mn_{0.2}Te_6$ sample are the same as those of the Ag_8GeTe_6 ternary compound; the sole exception is the reflection at 28.8°, which corresponds to $MnTe_2$ [14]. However, since its amount is small, this reflection is weak. The results of elemental analyses with a scanning electron microscope correspond to the composition of the solid solution.

Measurements of the Hall coefficient and the thermal emf in the 100–650 K temperature range revealed that the studied crystals were *p*-type.

Figure 2 presents the temperature dependences of the electric conductivity of $Ag_8Ge_{1-x}Mn_xTe_6$ alloys. All samples have high resistance values below the transition at 180–220 K. The electric conductivity increases in the

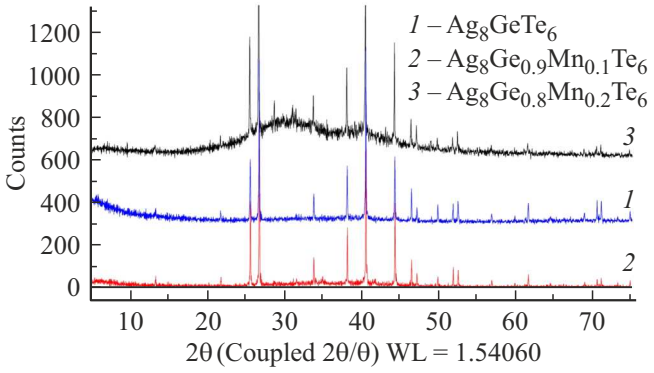

Figure 1. X-ray diffraction patterns of the $Ag_8Ge_{1-x}Mn_xTe_6$ solid solution.

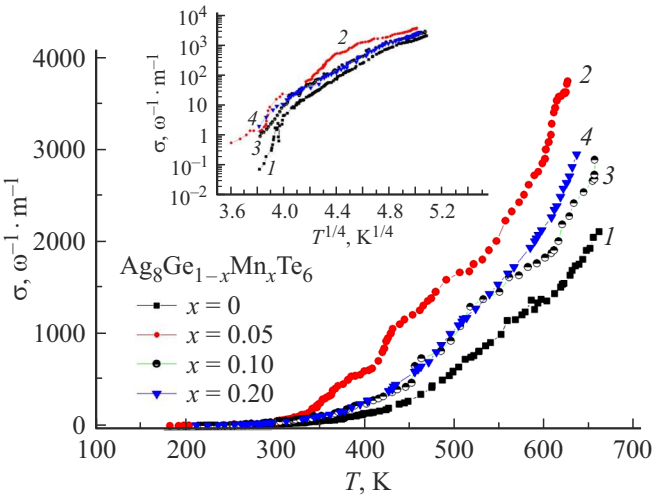

Figure 2. Electric conductivity of the $Ag_8Ge_{1-x}Mn_xTe_6$ solid solution. Dependence $\ln\sigma(T^{1/4})$ is shown in the inset.

220–300 K interval and varies in a semiconductor fashion in all compositions at $T > 320$ K.

According to the Mott theory [15,16], electric conduction in the 220–300 K interval is established by hopping from a localized state in a narrow energy band close to the Fermi level. It should be noted that an exponential dependence of the conductivity on the impurity density is the primary experimental evidence of hopping conduction.

We have analyzed conductivity dependences $\sigma(T)$ in the 220–300 K temperature interval using the Mott relation [15–17]

$$\sigma(T) = \sigma_0 \exp\left[-\left(\frac{T_0}{T}\right)^{1/4}\right], \qquad (1)$$

where $T_0 = \beta/g(\mu)r^3k_B$, $g(\mu)$ is the density of localized states near the Fermi level, r is the radius of localized states, k_B is the Boltzmann constant, and β depends on the system dimension ($\beta = 21$ [18]). Linear Mott plots were obtained in a certain temperature range. Structural disordering, interstitial impurities, vacancies, and dislocations distort the periodicity of the crystal structure and produce localized states with an energy falling within the band gap of an ideal crystal.

The $\ln\sigma(T^{1/4})$ dependence is shown in the inset of Fig. 2. It is evident that the curves for solid solutions $Ag_8Ge_{1-x}Mn_xTe_6$ in the 220–300 K temperature interval follow Mott dependence (1). The value of T_0 is specified by the curve slope in $\ln\sigma(T^{1/4})$ coordinates. Using the presented experimental data, we calculated the density of localized states near the Fermi level for $Ag_8Ge_{1-x}Mn_xTe_6$: $g(\mu) = 1.378 \cdot 10^{18}\,\mathrm{eV}^{-1} \cdot \mathrm{cm}^{-3}$ ($x = 0$); $1.684 \cdot 10^{19}\,\mathrm{eV}^{-1} \cdot \mathrm{cm}^{-3}$ ($x = 0.05$); $6.381 \cdot 10^{18}\,\mathrm{eV}^{-1} \cdot \mathrm{cm}^{-3}$ ($x = 0.10$); and $3.274 \cdot 10^{19}\,\mathrm{eV}^{-1} \cdot \mathrm{cm}^{-3}$ ($x = 0.20$). The obtained values suggest that the charge transfer in the indicated temperature range is established by carrier

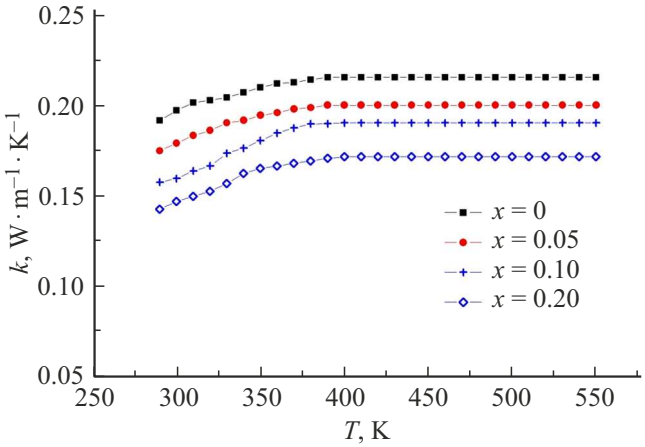

Figure 3. Thermal conductivity of the $Ag_8Ge_{1-x}Mn_xTe_6$ solid solution.

hopping between localized states in a narrow energy band near the Fermi level.

The thermal conductivity of samples was calculated based on temperature conductivity data for $T = 300-550$ K in accordance with the following formula: $k = \alpha\rho C_p$, where ρ is the density of the material and C_p is the thermal capacity of the sample (Fig. 3).

The contribution of carriers to the thermal conductivity calculated in accordance with the Wiedemann–Franz relation [19] increases from 10^{-3} to $6 \cdot 10^{-2}$ W/m · K, and its value is closer to the additional thermal conductivity.

$Ag_8Ge_{1-x}Mn_xTe_6$ solid solutions have a large number of atoms in a lattice cell (60 atoms) and thus feature more optical phonons in the phonon spectrum at higher temperatures. It is known that the anharmonicity of vibrations induces correlation of motion of atoms and atomic ensembles at equivalent points in the crystal lattice. The mechanism of propagation of vibrations in a crystal is disrupted as a result, each atom vibrates independently, and high-frequency vibrations become localized. It should be noted that the thermal conductivity in the „phonon-glass, electron-crystal" model depends on the crystal structure and the bond strength [20]. If a lattice cell is large and the average mass of atoms is high, a low thermal conductivity is to be expected. Calculating free path length l of phonons as

$$k = C_p v l/3, \qquad (2)$$

C_p — in accordance with the Dulong–Petit law

$$C_p\,(\mathrm{JK^{-1} \cdot mol^{-1}}) = 3n\mathrm{R}, \qquad (3)$$

where n is the number of atoms and $\mathrm{R} = 8.314\,\mathrm{JK^{-1} \cdot mol^{-1}}$ is the Rydberg number, and factoring in the values of thermal conductivity at room temperature ($k = 0.15-0.2\,\mathrm{W \cdot K^{-1} \cdot m^{-1}}$) and sound velocity in a crystal ($1750\,\mathrm{m \cdot s^{-1}}$ [10]), we find $l = 4.7-5.2$ Å. It is evident that the free path length of phonons is 2–3 times smaller than the lattice constant (11.58 Å [11]). The transfer of heat in a material where the free path of phonons does not exceed the lattice constant proceeds primarily via the energy exchange between neighboring atoms. Therefore, the temperature dependence of the thermal conductivity in such crystals is the same as the one in amorphous materials at higher temperatures.

Temperature dependences of the thermal emf of $Ag_8Ge_{1-x}Mn_xTe_6$ crystals are presented in Fig. 4. The observed reduction in thermal emf, which drops from 900 to 300 μV/K, at higher temperatures is typical of p-type semiconductors.

The thermoelectric figure of merit (ZT) for solid solutions $Ag_8Ge_{1-x}Mn_xTe_6$ was calculated based on the experimentally determined values of electric conductivity, thermal emf, and thermal conductivity. The results are presented in Fig. 5. It can be seen that the $Ag_8Ge_{0.95}Mn_{0.05}Te_6$ solution has the highest ZT, which reaches 0.7 at a temperature of 550 K. This value is 60% higher than the one corresponding to the nonstoichiometric $Ag_{8-x}GeTe_6$ ($x = 0,\ 0,\ 01$) composition, where $ZT = 0.4$ at 550 K [11].

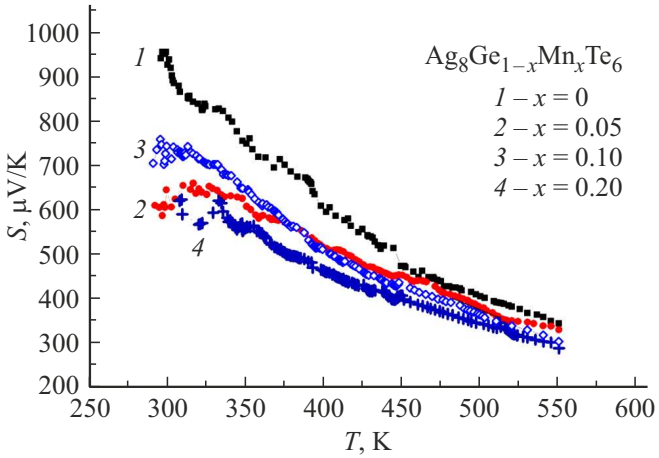

Figure 4. Seebeck coefficient of solid solution $Ag_8Ge_{1-x}Mn_xTe_6$.

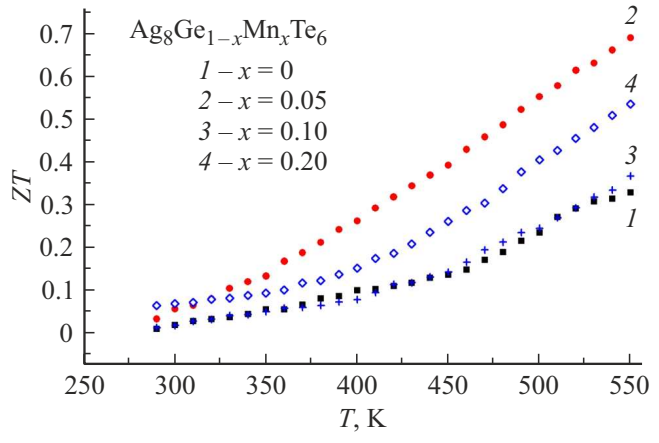

Figure 5. Thermoelectric figure of merit of solid solution $Ag_8Ge_{1-x}Mn_xTe_6$.

4. Conclusion

The structural equivalence of the studied *p*-type solid solutions $Ag_8Ge_{1-x}Mn_xTe_6$ ($x = 0$, 0.05, 0.1, 0.2) and the Ag_8GeTe_6 compound was established by X-ray diffraction analysis. It was demonstrated that the introduction of manganese induces compressibility of the Ag_8GeTe_6 lattice, and the emerging deformation field disrupts the lattice periodicity, thus enhancing the scattering of current carriers and phonons. The migration of ions also enhances the deformation field, and the free path length of phonons decreases as a result, becoming 2.5 times smaller than the lattice constant. The thermal conductivity of alloys is low due to the anharominicity of lattice vibrations. A high thermoelectric figure of merit $ZT = 0.7$ at 550 K was found for the $Ag_8Ge_{1-x}Mn_xTe_6$ ($x = 0.05$) solution.

Conflict of interest

The authors declare that they have no conflict of interest.

References

[1] D.M. Rowe (ed.). *CRC Handbook of Thermoelectrics* (CRC Press, N.Y., 1995).
[2] G. Jeffrey Snyder. Nature Mater., **7** (2), 105 (2008).
[3] M.S. Whittingham. MRS Bulletin, **14**, 31 (1989).
[4] F. Boucher, M. Evain, R. Brec. J. Solid State Chem., **107**, 332 (1993).
[5] R. Bendorius, A. Irzikevicius, A. Kindurys, E.V. Tsvetkova. Phys. Status Solidi A, **28**, K125 (1975).
[6] N. Rysanek, P. Laruelle, A. Katty. Acta Crystallogr., **B32**, 692 (1976).
[7] S. Geller. Zeitschrift. Kristallogr., **149**, 31 (1979).
[8] H. Kawaji, T. Atake. Solid State Ionics, **70/71**, 518 (1994).
[9] M. Fujikane, K. Kurosaki, H. Muta, S. Yamanaka. J. Alloys Compd., **396** (1), 280 (2005).
[10] A. Charoenphakdee, K. Kurosaki, H. Muta, M. Uno, S.Yamanaka. Phys. Status Solidi RRL, **2**, 65 (2008).
[11] T.J. Zhu, S.N. Zhang, S.H. Yang, X.B. Zhao. Phys. Status Solidi RRL, **4**, 317 (2010).
[12] W.J. Parker, R.J. Jenkins, C.P. Butler, G.L. Abbott. J. Appl. Phys., **32** (9), 1679 (1961).
[13] Aynur Gahramanova, Vagif Qasymov, Almaz Khalilova, Rashad Rahinov. *Proc. 7th Rostocker Int. Conf.: „Thermophysical Properties for Technical Thermodynamics"* (Rostock, Germany 2018) p. 73.
[14] Y. Xu, W. Li, C. Wang, Z. Chen, Y. Wu, X. Zhang, J. Li, S. Lin, Y. Chen, Y. Pei. J. Materiomics, **4**, 215 (2018).
[15] N.F. Mott. J. Non-Cryst. Solids, **1**, 1 (1968).
[16] N.F. Mott. Phil. Mag., **19**, 835 (1969).
[17] M.P. Fateev. Phys. Solid State, **52** (6), 1123 (2010).
[18] S.S. Ragimov, A.A. Saddinova, A.I. Alieva, R.I. Selim-zade. Inorg. Mater., **56** (8), 779 (2020).
[19] I.A Smirnov, V.I. Tamarchenko. *Elektronnaya teploprovodnost' v metallakh i poluprovodnikakh* (L., Nauka, 1977) (in Russian).
[20] G.A. Slack, D.W. Oliver, F.H. Horn. Phys. Rev. B, **4**, 1714 (1971).